Asian Journal of Physical and Chemical Sciences
1(2): 1-17, 2016; Article no.AJOPACS.31014

SCIENCEDOMAIN *international*
www.sciencedomain.org

The Numerical Study of Effects of Thermal Grashof Parameter and Concentration Grashof Parameter on Steady MHD Casson Fluid Flow through Non-Darcy Porous Media, over a Nonlinear Boundary Surface under Slip-conditions

Bhim Sen Kala[1*]

[1]*Koneru Lakshmaiah University, Guntur, 522502, A. P., India.*

Author's contribution

The sole author designed, analyzed and interpreted and prepared the manuscript.

Article Information

DOI: 10.9734/AJOPACS/2016/31014
Editor(s):
(1) Hesham Mansour, Physics Department, Faculty of Science, Cairo University, Egypt.
(2) Giannouli Myrsini, Department of Physics, University of Patras, Greece.
(3) Shridhar N. Mathad, Deptartment of Engineering Physics, KLE Institute of Technology, Karnataka, India.
Reviewers:
(1) P. A. Murad, LLC, Vienna, Virginia, USA.
(2) B. J. Gireesha, Kuvempu University, India.
Complete Peer review History: http://www.sciencedomain.org/review-history/17984

Original Research Article

Received 14th December 2016
Accepted 27th January 2017
Published 28th February 2017

ABSTRACT

In the present paper the numerical study of effects of thermal Grashof parameter and concentration Grashof parameter on steady MHD Casson fluid flow through non-Darcy porous media, over a nonlinear boundary surface under slip-conditions is explored. By suitable similarity transformations, the governing boundary layer equations are transformed to ordinary differential equations. The method of the numerical computation with bvp4c, a MATLAB program is applied to solve these equations. The effects of thermal Grashof, concentration Grashof and stretching index, velocity slip, thermal slip, and concentration slip parameters on velocity, heat transfer, and concentration profiles, Skin-friction, local Nusselt number and local Sherwood number are computed and discussed numerically and presented through tables and graphs.

**Corresponding author: E-mail: bhimskala@gmail.com;*

Keywords: Magnetohydrodynamics; Casson fluid, thermal Grashof number; slip parameters.

NOMENCLATURE AND SI UNITS

μ : dynamic viscosity($kgm^{-2}s^{-1}$)
υ : kinematic viscosity($m^{-2}s^{-1}$)
B : magnetic field(N/(mA))
H : convective heat transfer coefficient(W/m^2K)
c : Specific heat (J/kgK)
Cp : Specific heat at constant pressure
D : mass diffusivity(m^2s^{-1})
G : acceleration due to gravity (ms^{-2})
k : thermal conductivity(Wm^{-1} K^{-1})
m : mass kg
V : volume m^3
ρ : density kg/m^3
T : Temperature of fluid (K)
T : time(s)
u : horizontal component of velocity(m/s)
v : vertical component of velocity(m/s)
β : thermal expansion coefficient(K^{-1})
Gr_T : thermal Grashof number
Grc : mass(concentration) Grashof number
M : magnetic parameter
n : stretching index parameter
Nu : local Nusselt number
Pr : Prandtl number Prandtl number
Re : local Reynold number
Sc : Smidth number
Sh : local Sherwood number
C : concentration of fluid
x : distance along the plate distance along the plate
α : thermal diffusivity
η : similarity variable
x, y : Cartesian coordianates
θ : dimensionless temperature
ψ : Dimentiosless stream function

1. INTRODUCTION

Many natural, industrial as well as biological fluids (such as mud, condensed milk, glues, lubricating greases, paints, sugar solution, shampoos and tomato paste, polymers, liquid detergents, blood, fruit juices etc.) change their viscosity or flow behaviour under stress; and thus deviate from the classical Newton's law of viscosity. Different models of non-Newtonian fluids, based on their diverse flow behaviours have been discussed by the researchers.

The rheological model was introduced originally by Casson [1] in his research on a flow equation for pigment oil-suspensions of printing ink. Bird et al. [2] investigated the rheology and flow of visco-plastic materials. He reported that Casson model constitutes a plastic fluid model which exhibits shear thinning characteristics, yield stress, and high shear viscosity. Casson fluid behaves as solid when the shear stress is less than the yield stress and it starts to deform when shear stress becomes greater than the yield stress.

The fundamental analysis of the flow field of non-Newtonian fluids in a boundary layer adjacent to a stretching sheet or an extended surface is very important and is an essential part in the study of fluid dynamics and heat and mass transfer.

Sakiadis [3] studied boundary layer behaviour on continuous solid surfaces: II. The boundary layer on continuous flat surface. Crane [4] focused on the flow past a stretching plane. Nield et al. [5] investigated convection in porous media.

Mukhopadhyay [6] discussed Casson fluid flow and heat transfer over a nonlinearly stretching surface. Mustafa et al. [7] presented model for flow of Casson nanofluid past a non-linearly stretching sheet considering magnetic field effects. Medikare et al. [8] gave attention on MHD stagnation point flow of a Casson fluid over a nonlinearly stretching sheet with viscous dissipation.

Thermal radiation effects play important role in heat transfer control in polymer processing industry; the quality of final product depends on heat controlling factors. Pramanik [9] studied Casson fluid flow and heat transfer past an exponentially porous stretching surface in the presence of thermal radiation. Raju et al. [10] focused on heat and mass transfer in magnetohydrodynamic Casson fluid flow over an exponentially permeable stretching surface. Saidulu et al. [11] discussed slip effects on MHD flow of Casson fluid over an exponentially stretching sheet in presence of thermal radiation, heat source/sink and chemical reaction.

In chemical reactions, the rate of the chemical reaction depends upon the concentration of the species itself. A reaction rate is of nth order, if the reaction rate is proportional to the nth power of concentration. In particular, a reaction is of first order, if the rate is directly proportional to the concentration itself. Sharada et al. [12] investigated MHD mixed convection flow of a

casson fluid over an exponentially stretching surface with the effects of Soret, Dufour, thermal radiation and chemical reaction. Mukhopadhyay et al. [13] discussed exact solutions for the flow of Casson fluid over a stretching surface with transpiration and heat transfer effects. Hayat et al. [14] focused on Soret and Dufour effects on magnetohydrodynamic (MHD) flow of Casson fluid.

The mass flux created by temperature gradient is known as thermal –diffusion (Soret) effect and the energy flux created by temperature gradient is known as diffusion- thermo (Dufour) effect.

Mahdy [15] gave attention on heat transfer and flow of a Casson fluid due to a stretching cylinder with the Soret and Dufour effects. Animasaun [16] studied effects of thermophoresis, variable viscosity and thermal conductivity on free convective heat and mass transfer of non-Darcian MHD dissipative Casson fluid flow with suction and nth order of chemical reaction.

Ullah et al. [17] investigated effects of slip condition and Newtonian heating on MHD flow of Casson fluid over a nonlinearly stretching sheet saturated in a porous medium.

Some recent studies on the analysis of velocity, heat and mass transfer of Casson fluid flow can be found in Refs [18–31].

We consider (1) non-Darcy porous medium in momentum equation, (2) thermo-diffusion (Dufour) term in energy equation, (3) mass equation, (4) diffusion -thermo (Soret) term in the mass equation and (5) velocity slip factor, thermal slip factor, and mass slip factor in boundary conditions of velocity, temperature, and concentration, and (6) fluid flow over nonlinear surface respectively. In the study of references considered above, these terms simultaneously in one problem, are not investigated.

The present work is the extension of Ullah et al. [17] work by considering above terms.

It deals with the numerical study of effects of thermal Grashof parameter and concentration Grashof parameter on steady MHD Casson fluid flow through non-Darcy porous media, over a nonlinear boundary surface under slip-conditions.

2. MATHEMATICAL FORMULATION OF THE PROBLEM

In the formulation of the problem we consider following assumptions. Casson fluid is incompressible and electrically conducting. Flow is steady, laminar and two dimensional over a nonlinearly stretching sheet. Flow region is in non-Darcy porous medium. It is under the influence of transverse magnetic field B .The sheet is stretched nonlinearly along the x-axis (i.e. y=0) with velocity $u_w(x) = c\,x^n$;origin is taken as fixed and the fluid flow is confined to y>0. Here c is constant and $n(n \geq 0)$ is the nonlinear stretching index (sheet) parameter; $n = 1$ represents the linear sheet case and $n \neq 1$ is for nonlinear case; change in n (the stretching index parameter) affect the shape of the surface over which fluid flow occurs; shape of the surface has effect on the flow velocity, temperature and mass concentration of the fluid in the boundary layer region.

The magnetic Reynolds number of the flow is taken to be small enough so that induced magnetic field is assumed to be negligible in comparison with applied magnetic field so that $B = (0, B(x), 0),$ where $B(x)$ is the applied magnetic field, acting normal to the plate and varies in strength as a function of x. The flow is assumed to be in the x-direction which is taken along the plate and y-axis is normal to it. There is a constant suction/injection velocity v_w normal to the plate. The change in temperature produces the density variation and affects fluid flow; it is called thermal Grashof effect. The change in concentration produces the density variation and affects the fluid flow; it is called mass (concentration) Grashof effect. On the fluid flow, effect of temperature and concentration is also considered.

Under above assumptions the rheological equation for incompressible flow of Casson fluid is given by (Sharada et al. [12], Mukhopadhyay et al. [13])

$$\tau_{ij} = \begin{cases} 2(\mu_B + p_y / \sqrt{2\pi})e_{ij} & \pi > \pi_c \\ 2(\mu_B + p_y / \sqrt{2\pi_c})e_{ij} & \pi < \pi_c \end{cases},$$

where $\pi = e_{ij}\, e_{ij}$. And e_{ij} is the $(i,i) - \text{th}$ component of the deformation rate, π is the

product of the components of deformation, π_c is critical value of the product based on the non-Newtonian model, μ_B is the plastic dynamic viscosity of the non-Newtonian fluid, and p_y is the yield stress of the fluid. Yield stress is specific to a Casson fluid i.e. it depends upon the nature of fluid. Casson fluid behaves as solid when the shear stress is less than the yield stress and it starts to deform when shear stress becomes greater than the yield stress.

The viscosity and thermal conductivity of fluid are assumed to be constant. There is thermo-diffusion effect as well as diffusion-thermo effect. The pressure gradient, body forces and Joule heating are neglected compared with the effect of viscous dissipation. The temperature and concentration of the stretching surface are always greater than their free stream values. The flow configuration and the coordinate system are shown in Fig. 1.

Under the above assumptions and using Bossinesque approximation, boundary layer equations (Ullah et al. [17]) for flow with heat and mass transfer of Casson fluid are given by the following equations.

The continuity equation:

$$\frac{\partial u}{\partial x}+\frac{\partial v}{\partial y}=0\,, \tag{1}$$

The equation of momentum:

$$u\frac{\partial u}{\partial x}+v\frac{\partial u}{\partial y}=\upsilon\left(1+\frac{1}{\beta}\right)\frac{\partial^2 u}{\partial y^2}+g\beta_T(T-T_\infty)$$
$$+g\beta_C(C-C_\infty)-\frac{\sigma B^2(x)}{\rho}u-\frac{\upsilon}{K}u-\frac{b}{\sqrt{K}}u^2 \tag{2}$$

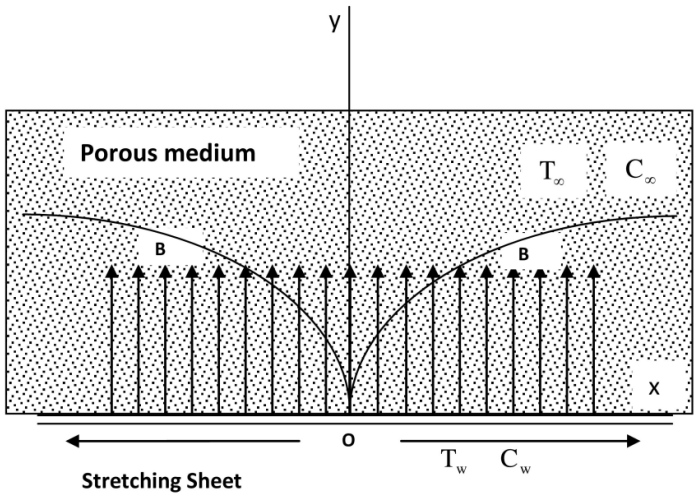

Fig. 1. Physical model and coordinate system

The Energy Equation:

$$u\frac{\partial T}{\partial x}+v\frac{\partial T}{\partial y}=\alpha\frac{\partial^2 T}{\partial y^2}+\left(\frac{D_m K_T}{C_S C_P}\right)\frac{\partial^2 C}{\partial y^2}+\frac{\mu}{\rho\, C_p}\left(1+\frac{1}{\beta}\right)\left(\frac{\partial u}{\partial y}\right)^2 \tag{3}$$

The Mass equation:

$$u\frac{\partial C}{\partial x}+v\frac{\partial C}{\partial y}=D_m\frac{\partial^2 C}{\partial y^2}+\left(\frac{D_m K_T}{T_M}\right)\frac{\partial^2 T}{\partial y^2} \tag{4}$$

where u and v are velocity components along x and y axes, respectively, ρ is fluid density, υ is kinematic viscosity, μ is dynamic viscosity, $\beta = \mu_B \sqrt{2\pi} / p_y$ is the Casson fluid parameter, σ is the electrical conductivity of the fluid which is assumed to be constant, β_T is coefficient of thermal expansion, β_C is coefficient of concentration expansion, T_W is temperature of the fluid at the stretching sheet, T is temperature of the fluid within the boundary layer, T_∞ is temperature of the fluid outside the boundary layer, k is thermal conductivity of the fluid, C_P is specific heat at constant pressure p, C_W is concentration of the fluid at the stretching sheet, C is concentration of the fluid within the boundary layer region, C_∞ is concentration of the fluid outside the boundary layer region, D_M is chemical molecular diffusivity. Here, g is acceleration due to gravity. The applied magnetic field is $B = B_0 x^{\frac{n-1}{2}}$, where B_0 is assumed to be constant.

Boundary conditions (Ullah et al. [17]):

$$At\ y = 0 : u = cx^n + N_1 \upsilon \left(1 + \frac{1}{\beta}\right)\frac{\partial u}{\partial y},\quad v = 0,\quad \frac{\partial T}{\partial y} = -h_s (T - T_w),\ \frac{\partial C}{\partial y} = -h_c (C - C_w)$$
$$As\ \ y \to \infty : u \to 0,\ T \to T_\infty,\ C \to C_\infty. \tag{5}$$

Here $N_1(x) = N x^{-\frac{n-1}{2}}$ denotes velocity of slip factor; it depends upon x. $h_s(x) = h_{T0}\, c\, x^{\frac{n-1}{2}}$ represents heat transfer parameter for Newtonian heating or temperature slip factor. And $h_c(x) = h_{c0}\, c\, x^{\frac{n-1}{2}}$ represents concentration slip factor.

2.1 Dimensional Analysis

We consider following dimensionless variable (Ullah et al. [17]) to transform the system of equations (2), (3), (4) and (5) into a dimensionless form:

$$\psi = \left(\frac{2\nu c}{n+1}\right)^{\frac{1}{2}} x^{\frac{n+1}{2}} f(\eta),\ \eta = \left(\frac{c(n+1)}{2\nu}\right)^{\frac{1}{2}} x^{\frac{n-1}{2}} y,\ \theta(\eta) = \frac{(T - T_\infty)}{(T_w - T_\infty)},\ \phi(\eta) = \frac{(C - C_\infty)}{(C_w - C_\infty)},$$
$$u = \frac{\partial \psi}{\partial y}, v = -\frac{\partial \psi}{\partial x},\ u = cx^n f'(\eta),\ v = -\left(\frac{c\upsilon(n+1)}{2}\right)^{\frac{1}{2}} x^{\frac{n+1}{2}} \left(f(\eta) + \frac{n-1}{n+1}\eta f'(\eta)\right) \tag{6}$$

Here, η is the similarity variable. ψ is stream function. $c\,(c > 0)$ is a parameter related to the surface stretching speed, n is the power index related to the surface stretching velocity.

Introducing these variables in the equations, (2), (3), (4) and (5) we get the following dimensionless forms of the equations:

$$(1 + \frac{1}{\beta}) f''' + f f'' + \frac{2n}{n+1} f'^2 + d_1 \theta + d_2 \phi - (M + (1/K_1)) f' - Fs\left(f'\right)^2 = 0 \tag{7}$$

$$\frac{1}{\mathrm{Pr}}\theta'' + f\theta' + \left(1 + \frac{1}{\beta}\right) Ec\, f''^2 = 0 \tag{8}$$

$$\frac{1}{Sc}\phi'' + f\,\phi' + Sr\,\theta'' = 0 \tag{9}$$

with parameters:

$$\left.\begin{aligned} &M = \frac{2\sigma B_0^2}{\rho c}, K1 = \frac{Kcx^{n-1}}{2\nu}, Fs = \frac{2bx}{\sqrt{K}}, \Pr = \frac{\upsilon}{\alpha} = \frac{\rho \upsilon C_p}{k} = \frac{\mu C_p}{k}, \\ &Gr_T = \frac{2g\beta_T (T_w - T_\infty)}{(n+1)c^2\, x^{2n-1}},\ Gr_C = \frac{2g\beta_C (C_w - C_\infty)}{(n+1)c^2\, x^{2n-1}}, u = cx^n \\ &Ec = \frac{u^2}{C_p (T_w - T_\infty)} = \frac{c^2 x^{2n}}{C_p (T_w - T_\infty)}' \nu = \frac{\mu}{\rho}, \\ &Sc = \frac{\upsilon}{D_m}, Du = \frac{D_m\ K_T\ (C_W - C_\infty)}{\upsilon\, C_S\, C_P\, (T_W - T_\infty)}, Sr = \frac{D_m\ K_T\ (T_W - T_\infty)}{\upsilon T_\infty\, (C_W - C_\infty)}. \end{aligned}\right\} \tag{10}$$

Here we consider following parameters with their symbols as follows:

M is magnetic parameter(Hartmann number), K1 is Permeability parameter, Fs is Forchheimer parameter, Pr is Prandtl number, Gr_T is thermal Grashof number, Gr_C is concentration Grashof number, Ec is Eckert number, Du is Dufour number, Sc is Schmidth number, Sr is Soret number.

And corresponding boundary conditions as follows:

$$\begin{aligned} &f(0) = 0, f'(0) = 1 + \delta\left(1 + \frac{1}{\beta}\right) f''(0), \theta'(0) = -\gamma_1 [1 + \theta(0)], \phi'(0) = -\gamma_2 [1 + \phi(0)] \\ &f'(\infty) = 0,\ \theta(\infty) = 0, \phi(\infty) = 0 \end{aligned} \tag{11}$$

where

$$\begin{aligned} &N = N_1\, x^{-\frac{n-1}{2}}, \delta = N\left(\frac{(n+1)c\upsilon}{2}\right)^{\frac{1}{2}},\ h_T = h_{T0}\, c\ x^{\frac{n-1}{2}}, \gamma_1 = h_{T0}\left(\frac{2\upsilon}{c(n+1)}\right)^{\frac{1}{2}} \\ &h_C = h_{C0}\, c\ x^{\frac{n-1}{2}}, \gamma_1 = h_{C0}\left(\frac{2\upsilon}{c(n+1)}\right)^{\frac{1}{2}} \end{aligned} \tag{12}$$

δ is called velocity slip parameter, γ_1 is called thermal slip parameter, and γ_2 is called concentration slip parameter.

The physical quantities of Engineering interest are the Skin-friction coefficient (rate of shear stress), the couple stress coefficient of the sheet, the local Nusselt number (rate of heat transfer), and the local Sherwood number (rate of mass transfer).

The Skin-friction C_f, local Nusselt Number Nu_x and local Sherwood Number Sh_x are defined as follows.

$$C_f = \frac{\tau_w}{\frac{\rho U_w^2}{2}}, Nu = -\frac{x\left(\frac{\partial T}{\partial y}\right)_{y=0}}{T_w - T_\infty}, Sh = -\frac{x\left(\frac{\partial C}{\partial y}\right)_{y=0}}{C_w - C_\infty}. \tag{13}$$

Using (6) and (13) we get

$$\left.\begin{aligned} C_f &= \frac{\tau_w}{\frac{\rho U_w^2}{2}} = \frac{\mu_B\left(1+\frac{1}{\beta}\right)\left(\frac{\partial u}{\partial y}\right)_{y=0}}{\frac{\rho U_w^2}{2}} \Rightarrow C_f = \left(\frac{2\nu(n+1)}{c}\right)^{\frac{1}{2}} x^{-\frac{(n+1)}{2}} f''(0), \\ C_f &= \left(\frac{2(n+1)}{\mathrm{Re}}\right)^{\frac{1}{2}}\left(1+\frac{1}{\beta}\right) f''(0),\ \mathrm{Re} = \frac{cx^{(n+1)}}{\nu}. \end{aligned}\right\} \tag{14}$$

$$\left.\begin{aligned} Nu &= -\frac{x\left(\frac{\partial T}{\partial y}\right)_{y=0}}{T_w - T_\infty} = -\left(\frac{c(n+1)}{2\nu}\right)^{\frac{1}{2}} x^{\frac{(n+1)}{2}} \theta'(0), \\ Nu &= -\left(\frac{(n+1)cx^{(n+1)}}{2\nu}\right)^{\frac{1}{2}} \theta'(0) = -\left(\frac{(n+1)}{2}\mathrm{Re}\right)^{\frac{1}{2}} \theta'(0). \end{aligned}\right\} \tag{15}$$

Here $-\left(\frac{\partial T}{\partial y}\right)_{y=0}$ is a heat flux from the surface of the sheet and Re is the local Reynold Number.

$$\left.\begin{aligned} Sh &= -\frac{x\left(\frac{\partial C}{\partial y}\right)_{y=0}}{C_w - C_\infty} = -\left(\frac{c(n+1)}{2\nu}\right)^{\frac{1}{2}} x^{\frac{(n+1)}{2}} \phi'(0), \\ Sh &= -\left(\frac{(n+1)cx^{(n+1)}}{2\nu}\right)^{\frac{1}{2}} \phi'(0) = -\left(\frac{(n+1)}{2}\mathrm{Re}\right)^{\frac{1}{2}} \phi'(0). \end{aligned}\right\} \tag{16}$$

Here $-\left(\frac{\partial C}{\partial y}\right)_{y=0}$ is a mass flow rate at the surface of the sheet and Re is the local Reynold number.

3. METHOD OF NUMERICAL SOLUTION

The numerical solutions are obtained using the equations (7)-(9) and boundary conditions (11) for some values of the governing parameters, namely, the thermal Grashof parameter (Gr_T), concentration Grashof parameter (Gr_C)and stretching index(sheet) parameter(γ_1), velocity slip parameter (δ), thermal slip parameter(γ_1) , and concentration slip parameter(γ_2). Effects of these parameters on the steady boundary layer flow are discussed in detail. The numerical computation is done using the MATLAB in-built

numerical solver bvp4c. In the computation we have taken $\eta_\infty = 10$ and axis according to the clear figure-visuality.

For convenience in calculation in Matlab, for parameter- symbols used in modelling equations and boundary conditions following symbols are used:

$$a1 = f''(0),\ a2 = \theta'(0),\ a3 = \phi'(0),\ d = \delta,$$
$$d1 = Gr_T,\ d2 = Gr_C,\ b = \beta,\ m1 = \gamma_1,\ m2 = \gamma_2,\ n1 = n.$$

4. RESULT ANALYSIS AND DISCUSSION

In order to analyze the behaviour of non-dimensional linear velocity $f'(\eta)$, temperature $\theta(\eta)$, and concentration $\phi(\eta)$ profiles of the physical problem, numerical calculations are carried out for various values of thermal Grashof parameter ($d1 = Gr_T$), concentration Grashof parameter ($d2 = Gr_C$)and stretching index parameter($m1 = \gamma_1$), velocity slip parameter ($d = \delta$), thermal slip parameter($m1 = \gamma_1$) , and concentration slip parameter($m2 = \gamma_2$). Also, the Skin-friction factor, local Nusselt number and local Sherwood number are discussed. For illustration of the results, the numerical data is tabulated in Tables 1-8 and plotted in Figs. 2–19.

The values of Skin-friction and local Nusselt number are compared with the previous published values, and are shown in Tables 1–2. It is observed that the obtained values are in good agreement with the published values.

Tables 1 and 2 present the values of Skin-friction coefficient and reduced Nusselt number for different values of nonlinear stretching parameter n and Prandtl number Pr, respectively. The present results are compared with the results of Cortell [18] and Ullah et al. [17]. It is observed from Table 1 that magnitude of Skin-friction coefficient $\left|\left(1+\frac{1}{b}\right)f''(0)\right|$ increases with the increase in n whereas reduced Nusselt number decreases with the increase in n and increases with the increase in Pr (Table 2).

Table 1. Comparison of $-f''(0)$ for different values of n1 with Fs=0.0, d1=0.0, d2=0.0, d=0.0, m1=10^4, m2=10^4, M=0, Pr=1.00, Du=0.0, Sc=0.22, a1=0.0, a2=1.0, a3=1.0, b=10^8, Ec=0.0, Da=10^7, Sr=0

	$-f''(0)$		
n1	**Cortell [18]**	**Ullah et al. [17]**	**Present values**
0.0	0.627547	0.6276	0.627631963479766
0.2	0.766758	0.7668	0.766906263551595
0.5	0.889477	0.8896	0.889594172073448
1	1.0	1.0	1.000062567556568
3	1.148588	1.1486	1.148660394543063
10	1.234875	1.2349	1.234952969673218
100	1.276768	1.2768	1.276830449563257

Table 2. Comparison of local Nusselt number $-\theta'(0)$ for various values of Pr and n1 with Fs=0.0, d1=0.0, d2=0.0, d=0.0, m1=10^4, m2=10^4, M=0, Pr=1.00, Du=0.0, Sc=0.22, a1=0.0, a2=1.0, a3=1.0, b=10^8, Ec=0.0, Da=10^7, Sr=0

	$-\theta'(0)$,Pr=1,		
n1	**Cortell [17]**	**Ullah et al. [18]**	**Present values**
0.2	0.610262	0.6102	0.610277445039946
0.5	0.595277	0.5949	0.595283487517005
1.5	0.574537	0.5747	0.574829838650739
3.0	0.564472	0.5647	0.564775152915357

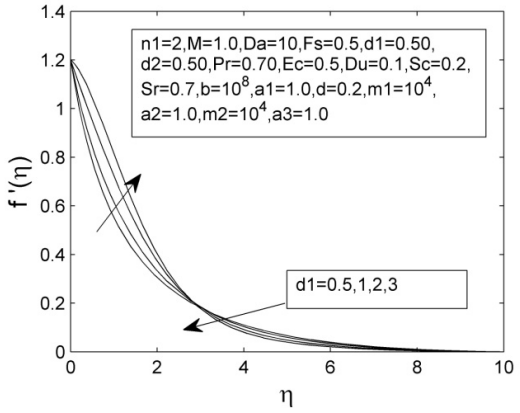

Fig. 2. Velocity profile $f'(\eta)$ with respect to similarity transformation η for some values of Thermal Grashof number d1

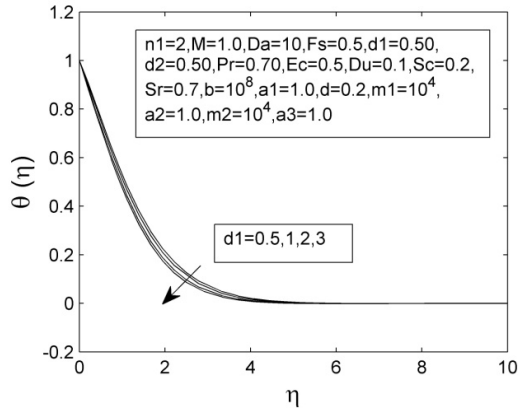

Fig. 3. Temperature profile $\theta(\eta)$ with respect to similarity transformation η for some values of Thermal Grashof number d1

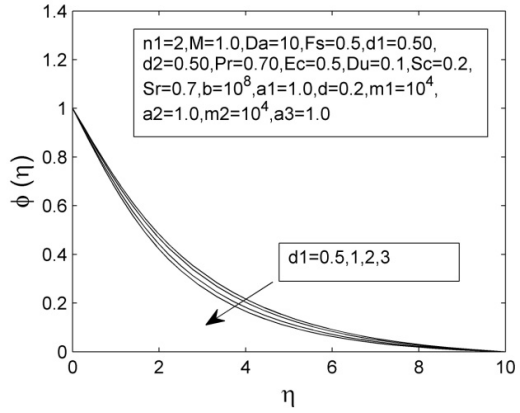

Fig. 4. Concentration profile $\phi(\eta)$ with respect to similarity transformation η for some values of Thermal Grashof number d1

It is shown in Fig. 2 that with the variation in the value of thermal Grashof number d1, the velocity profiles shows presence of point of intersection at some value of similarity variable in its (similarity variable's) range. Before the point of intersection velocity profiles increase and after the point of intersection velocity profiles decrease with the increase in d1 and thus causes thickening before the point of intersection and thinning after the point of intersection of the corresponding boundary layers.

Fig. 3 shows the behaviour of temperature profiles for increasing values of thermal Grashof number d1. The increasing values of d1 decrease the fluid temperature and leads to a decrease in thermal diffusion and results in thinning boundary layer.

Fig. 4 shows the behaviour of concentration profiles for increasing values of thermal Grashof number d1. The increasing values of d1 decrease the fluid concentration and leads to decrease in concentration diffusion and results in thinning boundary layer.

Fig. 5 shows the behaviour of velocity profile for increasing values of concentration Grashof number d2. The increasing values of d2 increase the fluid velocity and results in thickening boundary layer.

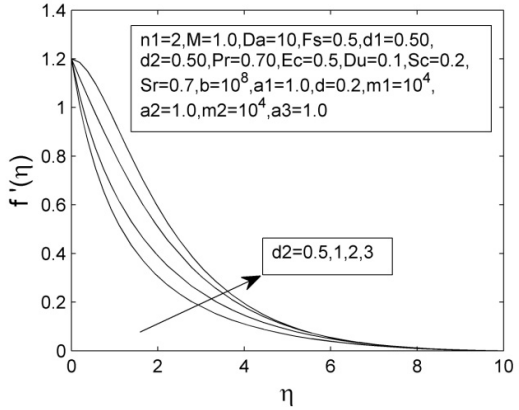

Fig. 5. Velocity profile $f'(\eta)$ with respect to similarity transformation η for some values of Concentration Grashof number d2

Fig. 6 shows the behaviour of temperature profiles for increasing values of concentration Grashof number d2. The increasing values of d2 decrease the fluid temperature and leads to

decrease in thermal diffusion and results in thinning boundary layer.

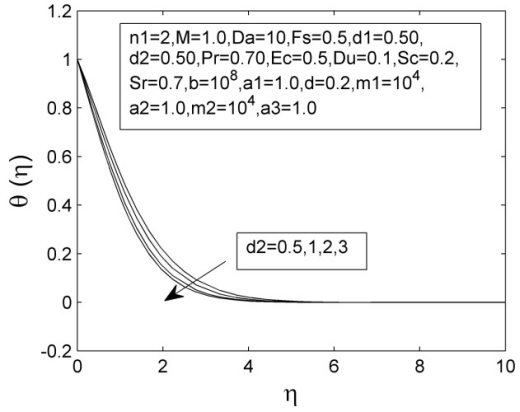

Fig. 6. Temperature profile $\theta(\eta)$ with respect to similarity transformation η for some values of Concentration Grashof number d2

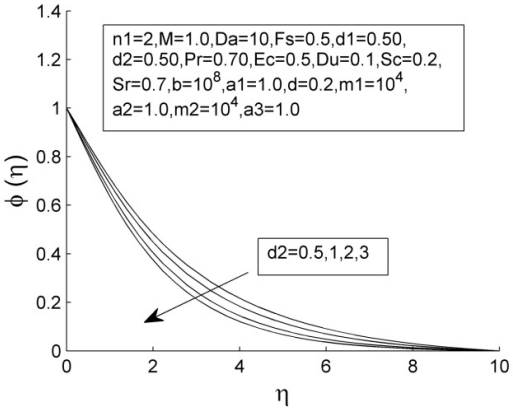

Fig. 7. Concentration profile $\phi(\eta)$ with respect to similarity transformation η for some values of Concentration Grashof number d2

Fig. 7 shows the behaviour of concentration profiles for increasing values of concentration Grashof number d2. The increasing values of d2 decrease the fluid concentration and leads to a decrease in mass diffusion and results in thinning boundary layer.

Fig. 8 shows the behaviour of velocity profile for increasing values of stretching index parameter n1. The increasing values of n1 increase the fluid velocity and leads to an increase in velocity and results in thickening boundary layer.

Fig. 9 shows the behaviour of temperature profiles for increasing values of stretching index parameter n1. The increasing values of n1 decrease the fluid temperature and leads to a decrease in thermal diffusion and results in thinning boundary layer.

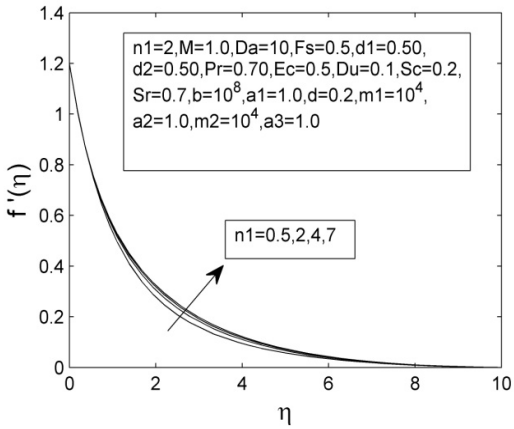

Fig. 8. Velocity profile $f'(\eta)$ with respect to similarity transformation η for some values of Stretching Index parameter n1

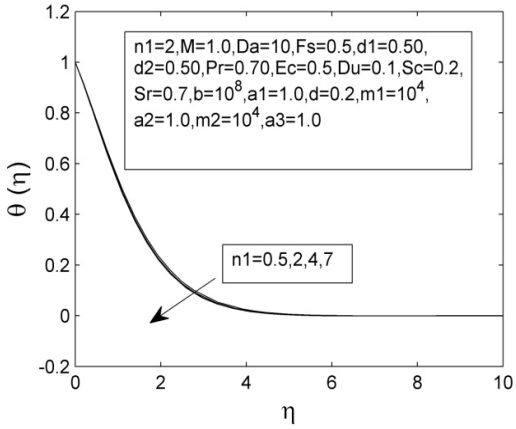

Fig. 9. Temperature profile $\theta(\eta)$ with respect to similarity transformation η for some values of stretching index parameter n1

Fig. 10 shows the behaviour of concentration profiles for increasing values of stretching index parameter n1. The increasing values of n1 decrease the fluid concentration and leads to decrease in mass diffusion and results in thinning boundary layer.

It is shown in Fig. 11 that with the variation in the value of velocity slip parameter d, the velocity profiles show presence of point of intersection at

some value of similarity variable in its (similarity variable's) range. Before the point of intersection velocity profiles increase and after the point of intersection velocity profiles decrease with the increase in d and thus causes thickening before the point of intersection and thinning after the point of intersection of the corresponding boundary layer.

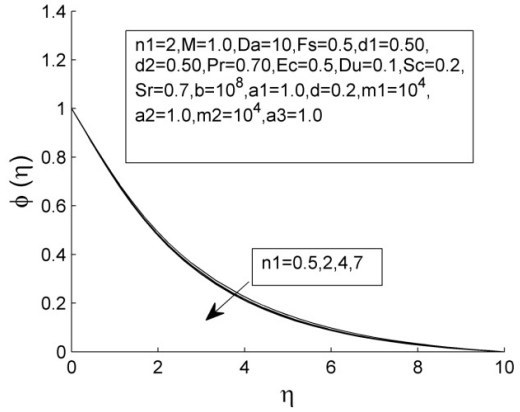

Fig. 10. Concentration profile $\phi(\eta)$ with respect to similarity transformation η for some values of stretching index parameter n1

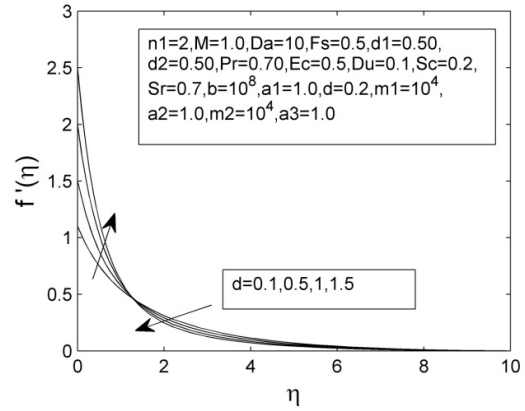

Fig. 11. Velocity profile $f'(\eta)$ with respect to similarity transformation η for some values of velocity slip parameter d

It is shown in Fig. 12 that with the variation in the value of velocity slip parameter, the temperature profiles show presence of point of inflexion at some value of similarity variable in its (similarity variable's) range. Before the point of inflexion temperature profiles increase and after the point of inflexion temperature profiles decrease with the increase in velocity slip parameter and thus causes thickening before the point of inflexion and thinning after the point of inflexion of the corresponding boundary layer.

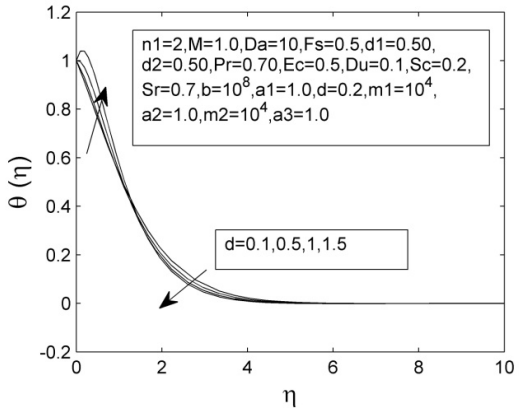

Fig. 12. Temperature profile $\theta(\eta)$ with respect to similarity transformation η for some values of velocity slip parameter d

Fig. 13 shows the behaviour of concentration profiles for increasing values of velocity slip parameter d. The increasing values of d decrease the fluid concentration and leads to decrease in mass diffusion and results in thinning boundary layer.

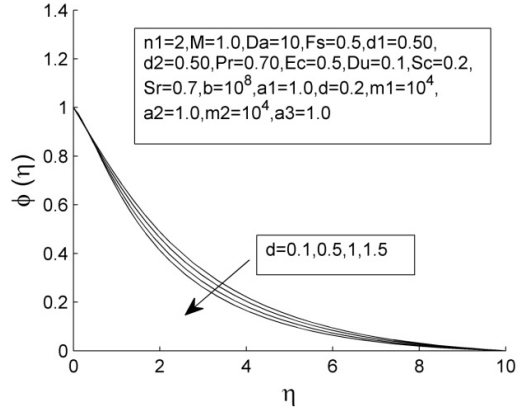

Fig. 13. Concentration profile $\phi(\eta)$ with respect to similarity transformation η for some values of velocity slip parameter d

It is shown in Fig. 14 that with the variation in the value of thermal slip parameter, the temperature profiles show presence of point of inflexion at some value of similarity variable in its (similarity

variable's) range. Before the point of inflexion temperature profiles decrease and after the point of inflexion temperature profiles increase with the increase in thermal slip parameter and thus causes thinning before the point of inflexion and thickening after the point of inflexion of the corresponding boundary layer.

Fig. 15 shows the behaviour of concentration profiles for increasing values of thermal slip parameter m1. The increasing values of m1 decrease the fluid concentration and leads to a decrease in mass diffusion and results in thinning boundary layer.

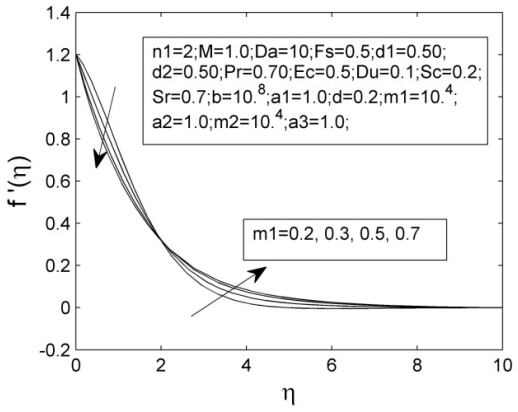

Fig. 14. Velocity profile $f'(\eta)$ with respect to similarity transformation η for some values of thermal slip parameter m1.

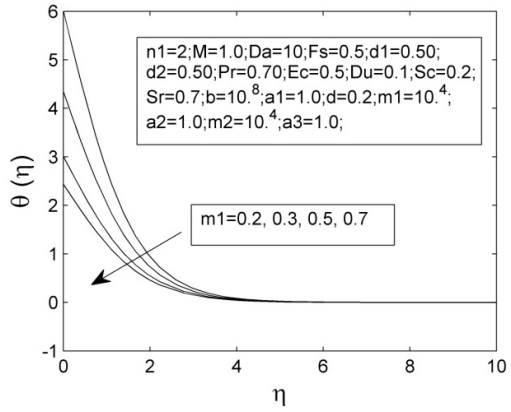

Fig. 15. Temperature profile $\theta(\eta)$ with respect to similarity transformation η for some values of thermal slip parameter m1

Fig. 16 shows the behaviour of concentration profile for increasing values of thermal slip parameter m1. The increasing values of m1 increase the fluid concentration and leads to increase in mass diffusion, and results in thickening boundary layer.

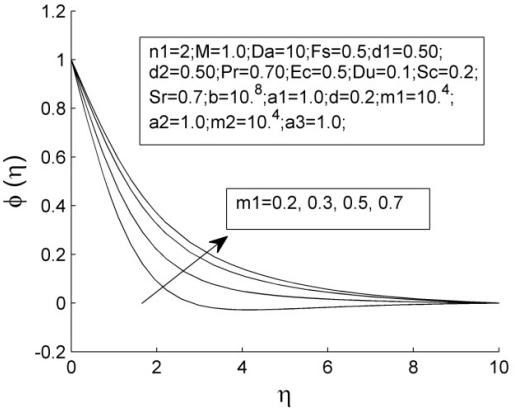

Fig. 16. Concentration profile $\phi(\eta)$ with respect to similarity transformation η for some values of thermal slip parameter m1

It is shown in Fig. 17 that with the variation in the value of concentration slip parameter m2, the velocity profiles show presence of point of inflexion at some value of similarity variable in its (similarity variable's) range. Before the point of inflexion velocity profiles attain maxima and after the point of inflexion velocity profiles decrease with the increase in concentration slip parameter m2 and thus causes thickening before the point of inflexion and thinning after the point of inflexion of the corresponding boundary layer.

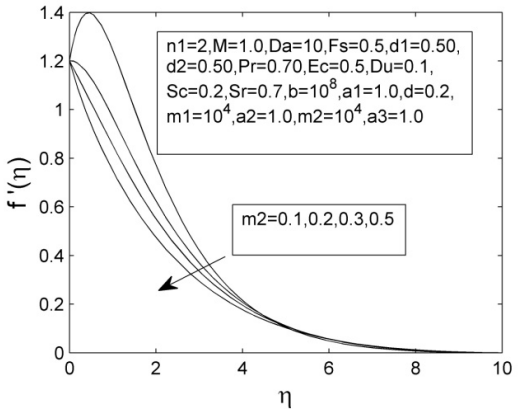

Fig. 17. Velocity profile $f'(\eta)$ with respect to similarity transformation η for some values of concentration slip parameter m2

Fig. 18 shows the behaviour of temperature profile for increasing values of concentration slip parameter m2. The increasing values of m2 increase the fluid temperature and leads to a increase in thermal diffusion and results in thickening boundary layer.

Fig. 19 shows the behaviour of concentration profiles for increasing values of concentration slip parameter m2. The increasing values of m2 decrease the fluid concentration and leads to a decrease in concentration diffusion and results in thinning boundary layer.

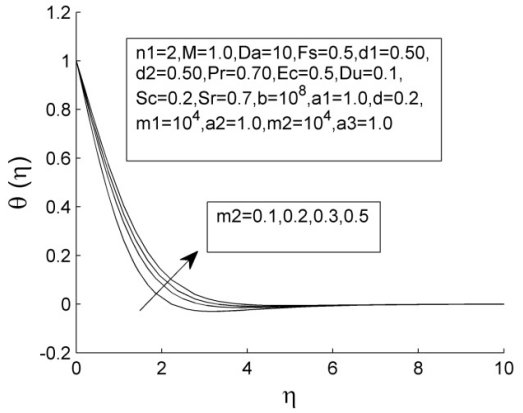

Fig. 18.Temperature profile $\theta(\eta)$ with respect to η similarity transformation for some values of concentration slip parameter m2

Table 3 shows with the increase in thermal Grashof number, Skin-friction decreases, local Nusselt number and local Sherwood number increase.

Table 4 shows with the increase in concentration Grashof number Skin-friction decreases, local Nusselt number and local Sherwood number increase.

Table 5 shows with the increase in stretching index parameter Skin-friction decreases, local Nusselt number and local Sherwood number increase.

Table 6 shows with the increase in velocity slip parameter, Skin-friction, local Nusselt number and local Sherwood number decreases.

Table 7 shows with the increase in thermal slip parameter, Skin-friction, local Nusselt number and local Sherwood number decrease.

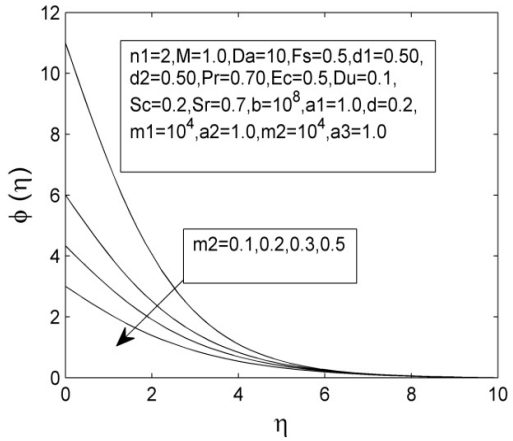

Fig. 19. Concentration profile $\phi(\eta)$ with respect to similarity transformation η for some values of concentration slip parameter m2

Table 8 shows with the increase in concentration slip parameter, Skin-friction, local Nusselt number and local Sherwood number decrease.

Table 3. Comparison of local Skin-friction $f''(0)$, local Nusselt number $-\theta'(0)$, and local Sherwood number $-\phi'(0)$ for various values of Thermal Grashof parameter d1

n1=2;M=1.0;Da=10;Fs=0.5;d1=0.50;d2=0.50;Pr=0.70;Ec=0.5;Du=0.1;Sc=0.2; Sr=0.7;b=10^8;a1=1.0;d=0.2;m1=10^4;a2=1.0;m2=10^4;a3=1.0			
d1	$f''(0)$	$-\theta'(0)$	$-\phi'(0)$
0.5	-1.139171110747207	0.412286376828377	0.291199312367934
1	-0.924674698901373	0.463136960151034	0.307607467201971
2	-0.520262779220773	0.533736823794359	0.333044041642291
3	-0.136273342804153	0.575792046556303	0.352221016180282

Table 4. Comparison of local Skin-friction $f''(0)$, local Nusselt number $-\theta'(0)$, and local Sherwood number $-\phi'(0)$ for various values of Concentration Grashof parameter d2

n1=2;M=1.0;Da=10;Fs=0.5;d1=0.50;d2=0.50;Pr=0.70;Ec=0.5;Du=0.1;Sc=0.2; Sr=0.7;b=10^8;a1=1.0;d=0.2;m1=10^4;a2=1.0;m2=10^4;a3=1.0			
d2	$f''(0)$	$-\theta'(0)$	$-\phi'(0)$
0.5	-1.139171110747207	0.412286376828377	0.291199312367934
1	-0.889855912405966	0.490721434531348	0.321141516623845
2	-0.429058096774202	0.588161328040350	0.361560777019338
3	-0.000005215126383	0.639622713232535	0.388558943654556

Table 5. Comparison of local Skin-friction $f''(0)$, local Nusselt number $-\theta'(0)$, and local Sherwood number $-\phi'(0)$ for various values of Stretching Index parameter n1

n1=2;M=1.0;Da=10;Fs=0.5;d1=0.50;d2=0.50;Pr=0.70;Ec=0.5;Du=0.1;Sc=0.2; Sr=0.7;b=10^8;a1=1.0;d=0.2;m1=10^4;a2=1.0;m2=10^4;a3=1.0			
n1	$f''(0)$	$-\theta'(0)$	$-\phi'(0)$
0.5	-1.107834524593921	0.400034622223237	0.285095245862456
2	-1.139171110747207	0.412286376828377	0.291199312367934
4	-1.151827273795374	0.417067365072081	0.293706192937322
7	-1.158981410957736	0.419716940271576	0.295129581837988

Table 6. Comparison of local Skin-friction $f''(0)$, local Nusselt number $-\theta'(0)$, and local Sherwood number $-\phi'(0)$ for various values of Velocity Slip parameter d

n1=2;M=1.0;Da=10;Fs=0.5;d1=0.50;d2=0.50;Pr=0.70;Ec=0.5;Du=0.1;Sc=0.2; Sr=0.7;b=10^8;a1=1.0;d=0.2;m1=10^4;a2=1.0;m2=10^4;a3=1.0			
d	$f''(0)$	$-\theta'(0)$	$-\phi'(0)$
0.1	-0.937342673670912	0.438194038419332	0.290086238282107
0.5	-1.783355656099067	0.288247163113478	0.287866635350244
1	-2.977042314559305	-0.085854377106689	0.258461876416481
1.5	-4.307781126641889	- 0.690959162359931	0.196506250870556

Table 7. Comparison of local Skin-friction $f''(0)$, local Nusselt number $-\theta'(0)$, and local Sherwood number $-\phi'(0)$ for various values of Thermal Slip parameter m1

n1=2;M=1.0;Da=10;Fs=0.5;d1=0.50;d2=0.50;Pr=0.70;Ec=0.5;Du=0.1;Sc=0.2; Sr=0.7;b=10^8;a1=1.0;d=0.2;m1=10^4;a2=1.0;m2=10^4;a3=1.0			
m1	$f''(0)$	$-\theta'(0)$	$-\phi'(0)$
0.1	0.610103383798474	7.153388196192017	1.120671503628536
0.2	-0.213885449511540	3.699042263686635	0.682247981827339
0.3	-0.508142098592084	2.560199251966306	0.547811963356730
0.5	-0.752540753371500	1.677252362446840	0.443148025627339

Table 8. Comparison of local Skin-friction $f''(0)$, local Nusselt number $-\theta'(0)$, and local Sherwood number $-\phi'(0)$ for various values of Concentration Slip parameter m2

n1=2;M=1.0;Da=10;Fs=0.5;d1=0.50;d2=0.50;Pr=0.70;Ec=0.5;Du=0.1;Sc=0.2; Sr=0.7;b=10^8;a1=1.0;d=0.2;m1=10^4;a2=1.0;m2=10^4;a3=1.0			
m2	$f''(0)$	$-\theta'(0)$	$-\phi'(0)$
0.1	1.041439944747776	0.764447309403654	4.138061437710518
0.2	0.030578419285525	0.699488592506508	2.042683211959266
0.3	-0.333797749258752	0.641229843346451	1.408317575601098
0.5	-0.640354448487176	0.573650792771382	0.932251856191939

5. CONCLUSION

In the present paper the numerical study of effects of thermal Grashof parameter and concentration Grashof parameter on steady MHD Casson fluid flow through non-Darcy porous media, over a nonlinear boundary surface under slip-conditions, is explored. The effects of thermal Grashof number, concentration Grashof number and stretching index, velocity slip, thermal slip , and concentration slip parameters on velocity, heat transfer, and concentration profiles, Skin- frictions, local Nusselt number and local Sherwood number are computed and discussed numerically and presented through tables and graphs.

From the above work following results are concluded.

With the increase in each of magnetic parameter, Dufour parameter, Soret parameter, Casson parameter, Prandtl number, and Schmidth number, velocity profiles decrease and thus cause thinning of the corresponding boundary layers.

With the increase in each of thermal Grashof number, concentration Grashof number, stretching index parameter, thermal slip parameter, temperature profiles decrease and thus cause thinning of the corresponding boundary layers.

With the increase in thermal Grashof number, concentration Grashof number, stretching index parameter, velocity slip parameter, concentration slip parameter, concentration profiles decrease and thus cause thinning of the corresponding boundary layers.

With the increase thermal slip parameter, before the point of inflexion velocity profile decreases and after the point of inflexion velocity profile increases and thus causes thinning before the point of inflexion and thickening after the point of inflexion of the corresponding boundary layer.

With the increase in thermal Grashof number, and velocity slip parameter, before the point of intersection velocity profile increases and after the point of intersection velocity profile decreases and thus causes thickening before the point of intersection and thinning after the point of intersection of the corresponding boundary layer.

Velocity profiles increase and thus cause thickening of the corresponding boundary layers with the increase in concentration Grashof number, and stretching index parameter.

Temperature profiles increase and thus cause thickening of the corresponding boundary layers with the increase in concentration slip parameter.

Concentration profiles increase and thus cause thickening of the corresponding boundary layers with the increase in thermal slip parameter.

With the increase in the value of concentration slip parameter, velocity profiles show increase before the point of inflexion and decrease after the point of inflexion, and hence cause increase before the point of inflexion and decrease after the point of inflexion in the corresponding boundary layer thickness.

With the increase in the value of velocity slip parameter, temperature profiles show increase before the point of inflexion and decrease after the point of inflexion, and hence cause increase before the point of inflexion and decrease after the point of inflexion in the corresponding boundary layer thickness.

Skin -friction decreases, local Nusselt number and local Sherwood number increase with the

increase in thermal Grashof number, concentration Grashof number, and stretching index parameter.

Skin-friction, local Nusselt number and local Sherwood number decrease with the increase in velocity slip parameter, thermal slip parameter, concentration slip parameter.

COMPETING INTERESTS

Author has declared that no competing interests exist.

REFERENCES

1. Casson N. In: Mill CC, editor. A flow equation for pigment oil-suspensions of the printing ink type. Rheology of Disperse Systems, 84.Pergamon Press; 1959.
2. Bird RB, Dai GC, Yarusso BJ. The rheology and flow of viscoplastic materials. Rev Chem Eng. 1983;1:1–83.
3. Sakiadis BC. Boundary layer behavior on continuous solid surfaces: II. The boundary layer on continuous flat surface. AIChE J. 1961;7:221–225.
4. Crane LJ. Flow past a stretching plane. Z. Angew. Math. Phys. 1970;21:645–647.
5. Nield DA, Bejan A. Convection in porous media. 2nd ed. Springer, New York; 1999.
6. Mukhopadhyay Swati. Casson fluid flow and heat transfer over a nonlinearly stretching surface. Chin. Phys. B. 2013; 22(7):074701.
   DOI: 10.1088/1674-1056/22/7/074701
7. Mustafa M, Junaid Ahmad Khan. Model for flow of Casson nanofluid past a non-linearly stretching sheet considering magnetic field effects. AIP Advances. 2015;5:077148.
   DOI: http://dx.doi.org/10.1063/1.4927449
8. Medikare M, Joga S, Chidem KK. MHD stagnation point flow of a Casson fluid over a nonlinearly stretching sheet with viscous dissipation. American Journal of Computational Mathematics. 2016;6:37-48.
   DOI:http://dx.doi.org/10.4236/ajcm.2016.61005
9. Pramanik S. Casson fluid flow and heat transfer past an exponentially porous stretching surface in presence of thermal radiation. Ain Shams Engineering Journal. 2014;5:205–212.
   DOI:http://dx.doi.org/10.1016/j.asej.2013.05.003
10. Raju CSK, Sandeep N, Sugunamma V, Jayachandra Babu M, Ramana Reddy JV. Heat and mass transfer in magnetohydrodynamic Casson fluid over an exponentially permeable stretching surface. Engineering Science and Technology, an International Journal. 2016;19:45–52.
    DOI:http://dx.doi.org/10.1016/j.jestch.2015.05.010
11. Saidulu N, Venkata Lakshmi A. Slip effects on MHD flow of Casson fluid over an exponentially stretching sheet in presence of thermal radiation, heat source/sink and chemical reaction. European Journal of Advances in Engineering and Technology. 2016;3(1):47-55.
12. Sharada K, Shankar B. MHD mixed convection flow of a Casson fluid over an exponentially stretching surface with the effects of soret, dufour, thermal radiation and chemical reaction. World Journal of Mechanics. 2015;5:165-177.
    DOI:http://dx.doi.org/10.4236/wjm.2015.59017
13. Swati Mukhopadhyay, Krishnendu Bhattacharyya, Tasawar Hayat. Exact solutions for the flow of Casson fluid over a stretching surface with transpiration and heat transfer effects. Chin. Phys. B. 2013; 22(11):114701.
    DOI: 10.1088/1674-1056/22/11/114701
14. Hayat T, Shehzadi SA, Alsaedi A. Soret and dufour effects on magnetohydrodynamic (MHD) flow of Casson fluid. Appl Math Mech (English Ed.) 2012;33(10):1301–12.
15. Mahdy A. Heat transfer and flow of a Casson fluid due to a stretching cylinder with the soret and dufour effects. Journal of Engineering Physics and Thermophysics. 2015;88(4).
16. Animasaun IL. Effects of thermophoresis, variable viscosity and thermal conductivity on free convective heat and mass transfer of non-darcian MHD dissipative Casson fluid flow with suction and nth order of chemical reaction. Journal of the Nigerian Mathematical Society. 2015;34: 11–31.
    DOI:http://dx.doi.org/10.1016/j.jnnms.2014.10.008
17. Imran Ullah, Sharidan Shafie, Ilyas Khan, Effects of slip condition and Newtonian heating on MHD flow of Casson fluid over a nonlinearly stretching sheet saturated in

a porous medium. Journal of King Saud University–Science; 2016.
DOI:dx.doi.org/10.1016/j.jksus.2016.05.003

18. Cortell R. Viscous flow and heat transfer over a nonlinearly stretching sheet. App. Math.Comput. 2007;184:864-873.
19. Butt AS, Tufail MN, Asif Ali. Three-dimensional flow of a magnetohydro-dynamic Casson fluid over an unsteady stretching sheet embedded into a porous medium. Journal of Applied Mechanics and Technical Physics. 2016;57(2):283–292.
ISSN 0021-8944
20. Shehzad SA, Hayat T, Qasim M, Asghar S. Effects of mass transfer on MHD flow of Casson fluid with chemical reaction and suction. Brazilian Journal of Chemical Engineering. 2013;30(01):187-195.
21. Arthur EM, Seini IY, Bortteir LB. Analysis of Casson fluid flow over a vertical porous surface with chemical reaction in the presence of magnetic field. Journal of Applied Mathematics and Physics. 2015;3: 713-723.
DOI:http://dx.doi.org/10.4236/jamp.2015.36085
22. Hussanan Abid, Mohd Zuki Salleh, Razman Mat Tahar, Ilyas Khan. Unsteady boundary layer flow and heat transfer of a Casson fluid past an oscillating vertical plate with newtonian Heating. PLOSONE. 2014;9(10):e108763
Available:www.plosone.org
23. Kirubhashankar CK, Ganesh S, Mohamed Ismail A. Casson fluid flow and heat transfer over an unsteady porous stretching surface. Applied Mathematical Sciences. 2015;9(7):345–351.
DOI:http://dx.doi.org/10.12988/ams.2015.411988
24. Motahar Reza, Rajni Chahal, Neha Sharma. Radiation effect on MHD Casson fluid flow over a power-law stretching sheet with chemical reaction. World Academy of Science, Engineering and Technology International Journal of Chemical, Molecular, Nuclear, Materials and Metallurgical Engineering. 2016;10(5).
25. Siddiqui AM, Farooq AA, Rana MA. A mathematical model for the flow of a Casson Fluid due to Metachronal Beating of cilia in a tube. Hindawi Publishing Corporation, The Scientific World Journal. 2015;12.
Article ID 487819
DOI:http://dx.doi.org/10.1155/2015/487819
26. Shaw Sachin, Ganeswar Mahanta, Precious Sibanda. Non-linear thermal convection in a Casson fluid flow over a horizontal plate with convective boundary condition. Alexandria Engineering Journal 2016;55:1295–1304.
DOI:http://dx.doi.org/10.1016/j.aej.2016.04.020
27. Rao AS, Prasad VR, Reddy NB, B´eg OA. Heat transfer in a Casson rheological fluid from a semi-infinite vertical plate with partial slip. Wiley Periodicals, Inc. Heat Trans Asian Res; Published online in Wiley Online Library; 2013.
DOI:http://dx.doi.org/10.1002/htj.21115
Available:wileyonlinelibrary.com/journal/htj
28. Forchheimer PZ. Wasserbewegung Durch Boden. Zeit Ver Deutsch Ing. 1901;45: 1781–8.
29. Darcy H. Les fontainer publigues de la ville de Dijoin. Dalmont; 1856.
30. Krishnamurthy MR, Gireesha BJ, Prasannakumara BC, Gorla Rama Subba Reddy. Thermal radiation and chemical reaction effects on boundary layer slip flow and melting heat transfer of nanofluid induced by a nonlinear stretching sheet. Nonlinear Engineering. 2016;5(3):147-159.
DOI: 10.1515/nleng-2016-0013
31. Prasannakumara BC, Gireesha BJ, Gorla Rama SR, Krishnamurthy MR. Effects of chemical reaction and nonlinear thermal radiation on Williamson nanofluid slip flow over a stretching sheet embedded in a porous medium. Journal of Aerospace Engineering. 2016;29(5): 04016019.

Peer-review history:
The peer review history for this paper can be accessed here:
http://sciencedomain.org/review-history/17984